Technical Documentation of Renewable Energy Systems Co-benefits Assessment Tool RES-CAT

Energy and Environmental Systems (EES) Laboratory

Kyushu Univesity

The RES-CAT Back-End Engineering:

This section presents all the mathematical formulations and assumptions used in the design and development of the RES-CAT tool.

1. **Energy Balance**

The energy balance equation for all the RES resources is formulated based on Equation (1.a).

$$E_{PV_t} + E_{WT_t} + E_{BG_t} + E_{Grid\_Pur_t} + E_{BD_t} = E_{Grid\_Sell_t} + E_{BC_t} + E_{Load_t} \quad (1.a)$$

Where the first term represents the hourly electricity generated from the photovoltaics (E_{PV_t}). The second term represents the hourly electricity generated by the wind turbines (E_{WT_t}). The third term accounts for the hourly electricity produced by the biomass generators (E_{BG_t}). The fourth term depicts the hourly electricity purchased from the main grid ($E_{Grid\_Pur_t}$). The fifth term represents the hourly electricity discharged from the battery (E_{BD_t}). The sixth term denotes the hourly electricity sold to the main grid ($E_{Grid\_Sell_t}$). The seventh term indicates the hourly electricity charged into the battery (E_{BC_t}). Finally, the last term represents the hourly electricity load demand (E_{Load_t}).

2. **Solar PV Electricity Generation**

The RES-CAT tool PV electricity generation formulation adopts three key system aspects to ensure effectiveness and accuracy.

I. PV Array Technological Options

The RES-CAT tool considers four PV array technologies: Monocrystalline I, Monocrystalline II, Polycrystalline I, and Polycrystalline II, each with distinct technical specifications (capacity, efficiency, temperature coefficients).

II. Core Inputs & Performance Adjustments

The tool uses geographical data (location, tilt, orientation), meteorological data (radiation, temperature), and manufacturer specifications (capacity, derating factor, efficiency). In addition, hourly output is calculated by adjusting for cell temperature rise (up to 30°C above ambient), with performance corrected using the temperature coefficient and efficiency curves.

III. Detailed Irradiance and Solar Geometry Modeling

The tool advances beyond raw horizontal radiation data by calculating global tilted irradiance through the integration of beam, diffuse, and ground-reflected components. It further incorporates solar geometry parameters (declination, hour angle, anisotropy index, horizon brightening, albedo) alongside panel slope and azimuth orientation. This allows for precise, hourly estimation of PV output under real-world conditions, capturing the full effect of tilt, direction, and solar position on system performance. Figure 1 presents the adopted modeling framework for solar PV electricity generation. From the model, the input parameters to be defined by the user are the geographical data, meteorological data, the installed capacity, and the slope angle of the solar PV panel in degrees. The solar PV electricity generated is obtained from equation (2.a).

$$E_{PV} = Y_{PV} \cdot f_{PV} \cdot \left(\frac{\overline{G_T}}{\overline{G_{T,STC}}}\right) \cdot \left[1 + \alpha_p\left(T_C - T_{C,STC}\right)\right] \qquad (2.\mathrm{a})$$

where Y_{PV} is the rated capacity of the PV array in kW (i.e., the output power under standard test conditions of 1000W/m^2 luminous intensity, 25°C temperature, and 1.5 air mass). f_{PV} is the derating factor of the PV modules in percent. $\overline{G_T}$ is the incident solar radiation on PV arrays at the current time interval in kW/m^2. $\overline{G_{T,STC}}$ is the standard test condition of the incident radiation in kW/m^2. α_p is the power temperature coefficient in %/°C. T_C and $T_{C,STC}$ are the instantaneous PV cell temperature in Celsius and the standard test condition cell temperature at 25°C, respectively. The hourly precise calculation of T_C is expressed in Equation (2.b).

$$T_C = \frac{T_a + \left(T_{C,NOCT} - T_{a,NOCT}\right) \cdot \left(\frac{G_T}{G_{T,NOCT}}\right) \cdot \left(1 - \frac{\eta_{mp,STC} \cdot \left(1 - \alpha_p \cdot T_{C,STC}\right)}{\tau\alpha}\right)}{1 + \left(T_{C,NOCT} - T_{a,NOCT}\right) \cdot \left(\frac{G_T}{G_{T,NOCT}}\right) \cdot \left(\frac{\alpha_p \cdot \eta_{mp,STC}}{\tau\alpha}\right)} \qquad (2.b)$$

where T_a, $T_{C,NOCT}$, and $T_{a,NOCT}$ are the ambient temperature in Kelvin, nominal operating cell temperature of 317 Kelvin, and ambient temperature at NOCT of 293 Kelvin, respectively. G_T and $G_{T,NOCT}$ are the incident solar radiation on the PV array in kW/m^2 and NOCT solar radiation, which is defined as 0.8 kW/m^2, respectively. $T_{C,STC}$ is the cell temperature under standard test conditions at 298 Kelvin. τ and α are the transmittance of any material covering the PV array and the PV array absorptance of solar in percent, respectively. $\eta_{mp,STC}$ is the maximum power point efficiency of the PV array under standard conditions in percent, which is calculated using equation (2.c):

$$\eta_{mp,STC} = \frac{Y_{PV}}{A_{PV} \cdot G_{T,STC}} \tag{2.c}$$

where A_{PV} is the PV array surface in m^2, while $G_{T,STC}$ is equal to 1 kW/m^2.

The precise calculation of the hourly output power from PV arrays necessitates a specific determination of the incident solar radiation received on the tiled surface in the targeted cities of Japan. Although climate stations provide reliable radiation records, the provided records normally contain only the radiation of horizontal surfaces, which lacks data on tilted surfaces. Total incident radiation on the tilted plane consists of three components: reflected radiation, diffuse radiation, and beam radiation from the ground. Hence, $\overline{G_T}$, the global incident radiation on the PV array is calculated in equation (2.d).

$$\overline{G_T} = (\overline{G_b} + \overline{G_d} \cdot A_i) \cdot R_b + \overline{G_d} \cdot (1 - A_i)\left(\frac{1+\cos\beta}{2}\right)\left[1 + f\sin^3\left(\frac{\beta}{2}\right)\right] + \bar{G} \cdot \rho_g \cdot \left(\frac{1-\cos\beta}{2}\right) \tag{2.d}$$

where $\overline{G_b}$ and $\overline{G_d}$ are the beam radiation and the radiation diffused in kW/m^2, respectively. A_i is the anisotropy index. R_b is the ratio of the radiation of the beam on a tilted surface to the beam radiation on the horizontal surface, obtained using equation (2.e). The horizon brightening factor f is calculated using equation (2.f). ρ_g is the ground reflectance in percentage, which can also be referred to as the albedo. β is the slope of the surface in degrees.

$$R_b = \frac{\cos\theta}{\cos\theta_z} \tag{2.e}$$

$$f = \sqrt{\frac{\overline{G_b}}{\bar{G}}} \tag{2.f}$$

The notation $\bar{G}$ is the total of beam and diffuse radiation in kW/m^2, obtained by summing the beam and the diffuse radiations.

To calculate the anisotropy index using equation (2.g), $\overline{G_0}$, the averaged horizontal extraterrestrial radiation over the time interval in kW/m^2, and G_{on} is the normal extraterrestrial radiation in kW/m^2 shall be sequentially obtained using equations (2.h) and (2.i):

$$A_i = \frac{\overline{G_b}}{\overline{G_0}} \tag{2.g}$$

$$\overline{G_0} = \frac{12}{\pi} G_{on} \cdot \left[\cos\phi \cos\delta \left(\sin\omega_2 - \sin\omega_1 \right) + \frac{\pi(\omega_2 - \omega_1)}{180^{\circ}} \sin\phi \sin\delta \right] \tag{2.h}$$

$$G_{on} = G_{sc} \cdot \left(1 + 0.033 \cdot \cos\frac{360n}{365} \right) \tag{2.i}$$

where ω_1 and ω_2 are the hour angle at the start of the time interval and the hour angle at the close of the time interval in degrees, respectively. n is the day number in the year. G_{sc} is the solar constant of 1.367 kW/m^2. On the other hand, the formed slope angle between the panel surface, the horizontal axis, and the azimuth direction of the panel surface faces is given. Then, sequentially, the declination of the sun and the hour angle of the sun location in the sky are calculated using equations (2.j) and (2.k). For instance, if the obtained hour angle is equal to 15, the sun moves 15° per hour across the sky.

$$\delta = 23.45^{\circ} \cdot \sin\left(360^{\circ} \cdot \frac{284 + n}{365} \right) \tag{2.j}$$

$$\omega = (t_s - 12\text{hr}) \cdot 15 {}^{\circ}/_{\text{hr}} \tag{2.k}$$

where δ is the declination of the sun in degrees. n is the day number in the year. ω is the hour angle in degrees. t_s is the solar time in hours, which can be obtained using equation (2.l). This necessitates an advanced calculation for the equation of time as expressed in (2.m):

$$t_s = t_c + \frac{\lambda}{15^{\circ}/\text{hr}} - Z_C + E \tag{2.l}$$

$$(2.m)$$

$$E = 3.82(0.000075 + 0.001868 \cdot \cos B - 0.032077 \cdot \sin B - 0.014615 \cdot \cos 2B - 0.04089 \cdot \sin 2B)$$

$$B = 360° \cdot \frac{(n-1)}{365} \qquad (2.n)$$

where t_c is the civil time in hourly intervals, which corresponds to the time intervals' midpoint. λ is the location's longitude in degrees. Z_C is the east of GMT time zone in hours. E is the equation of time in hours. Eventually, the angle of incidence can be obtained for any surface orientation using equation (2.n) as follows:

$$\cos\theta = \sin\delta \cdot \sin\phi \cdot \cos\beta - \sin\delta \cdot \cos\phi \cdot \sin\beta \cdot \cos\gamma + \cos\delta \cdot \cos\phi \cdot \cos\beta \cdot \cos\omega + \cos\delta \cdot \sin\phi \cdot \sin\beta \cdot \cos\gamma \cdot \cos\omega + \cos\delta \cdot \sin\beta \cdot \sin\gamma \cdot \sin\omega \qquad 2.p)$$

where θ, β, and γ are the angle of incidence, the slope of the surface, and the azimuth of the surface in degrees, respectively. ϕ, δ, and ω are the latitude, solar declination, and hour angle in degrees, respectively. θ_z is the zenith angle in degrees, which can be obtained using equation (2.p).

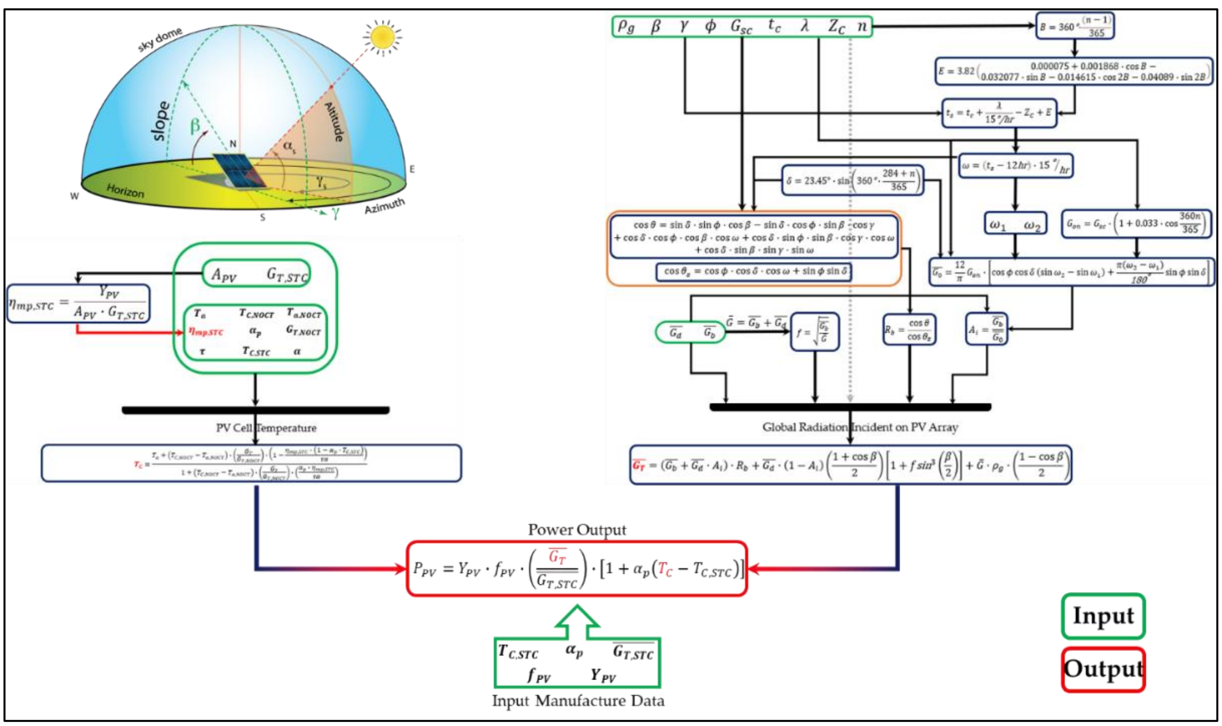

Figure 1: The modeling methodology for estimating solar PV electricity [1]

3. Wind Turbines Electricity Generation

This tool consists of 379 classifications of wind turbines per manufacturer: rated capacity, blade diameter, rated velocity, and cut-in velocity. The turbines were configured to generate the maximum power at the minimum wind speed. In this model, the ideal condition where the turbine blades capture all flowing wind is expressed in the equivalent electric power output using equation (3.a).

$$E_{WTt} = C_p P_{in} \tag{3.a}$$

where P_o is the electric power output from the wind turbine. C_p denotes the coefficient of power due to the wind turbine rotor's aerodynamic efficiency, which is a function of the tip speed ratio and pitch angle. P_{in} is the mechanical wind power harnessed by the turbine as calculated using equation (3.b). This relies on the Rankine–Froude model, accounting for rotational flow with emphasis on propellers; the power through a cross-sectional area is normal to the swept wind by the rotor blades. Equation (3.c) expresses the substitution of the harnessed wind mechanical power of (3.b) into (3.c), considering the tip speed ratio and pitch angle.

$$P_{in} = \frac{1}{2}\rho A v^3 \tag{3.b}$$

$$E_{WTt} = \frac{1}{2}C_p(\lambda, \beta)\rho A v^3 \tag{3.c}$$

where ρ is the air density. A is the blades' swept area. v is the wind speed in m/s. λ and β are the tip speed ratio and pitch angle, respectively. The tip speed ratio can be obtained using the ratio between the fringe speed of the blades and the wind speed, as expressed in equation (3.d).

$$\lambda = \frac{\Omega R}{v} \tag{3.d}$$

where Ω is the rotational speed of the blades in radians per second. R is the blade radius, and v is the free stream velocity of the wind. The value of the power coefficient as a function of tip speed ratio and pitch angle can be obtained as expressed in equation (3.f).

$$C_p(\lambda, \beta) = 0.5176\left(\frac{116}{\lambda_i} - 0.4\beta - 5\right)e^{\frac{-21}{\lambda_i}} + 0.0068\lambda \tag{3.f}$$

$$\frac{1}{\lambda_i} = \frac{1}{\lambda + 0.08\beta} - \frac{0.035}{\beta^3 + 1} \quad (3.g)$$

The total wind power is extracted according to the specified wind turbine type, where the wind speed of a given location at reference height, cut-in speed (i.e., minimum limit of electricity generation), cut-out speed (i.e., the maximum limit of electricity generation), and rated speed are given. This is mathematically calculated using equation (3.h).

$$P_{wind} = \begin{cases} E_{WTt}\left(\frac{v - v_{Cin}}{v_r - v_{Cin}}\right), & v_{cin} \le v \le v_r \\ E_{WTt}, & v_r \le v \le v_{Co} \\ 0, & v \le v_{Cin}, v \ge v_{Co} \end{cases} \quad (3.h)$$

$$v = v_{ref}\left(\frac{H}{H_{ref}}\right)^{\alpha} \quad (3.i)$$

where P_{wind} is the total generated electric power in kWh. v refers to the wind speed in meters per second for the defined height of H. v_{cin}, v_{Co}, and v_r refer to the cut-in speed, cut-out speed, and rated wind speed in meters per second, respectively. v_{ref} denotes the measured wind speed at the reference height in meters. The hourly generated wind power according to a given wind turbine type and manufacturer datasheets for a given location is calculated. The modeling equations of the overall power generated from the wind turbines are shown in **Figure** .

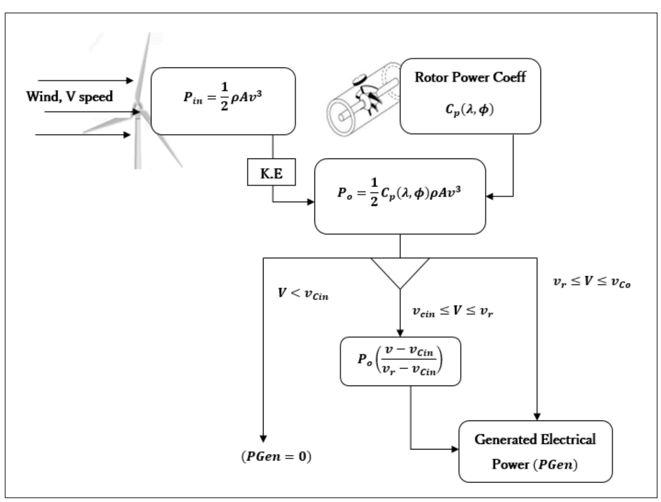

Figure 2: Overall power generation for the wind turbine.

4. Biomass Electricity Generation

The tool offers two types of biomass electricity supply technologies based on the feedstock categories. These are classified into the combustion of wood and agricultural feedstocks and waste-to-energy (WtE) incineration technology using municipal solid waste (MSW). The biomass electricity supply is estimated as modeled in [2]. However, the modeling approach is specifically customized to align with the overall HRES objective. In this model, the parameters are geographical information, meteorological data, biomass feedstock type, generation plant capacity, and combustion system. The energy and mass balance are modeled to obtain the hourly electricity output from biomass.

Feedstock Type:

The elemental composition of the biomass feedstock, mass fraction, net calorific value (i.e., low heating value (LHV)), gross calorific value (i.e., high heating value (HHV)), and dry-basis moisture content of the selected feedstock type are obtained. The model imports the feedstock's elemental composition and dry moisture content based on the given geographical location and feedstock type. The monthly ambient temperature and relative humidity are calculated using equations (4.a) and (4.b), respectively.

$$T_A = \frac{\sum_{n=0}^{N\times 24} T_n}{N \times 24} \quad (4.a)$$

$$r = \frac{\sum_{n=0}^{N\times 24} r_n}{N \times 24} \quad (4.b)$$

where T_A is the ambient temperature in Celsius. T_n is the temperature of the nth hour of the month in Celsius. n is the number of monthly hours, while N denotes the number of days in the month. r is the relative humidity in percent, and r_n is the relative humidity of the nth hour of the month in percent. The wet basis moisture content of the specified feedstock is calculated using equation (4.c), while the elemental composition of the feedstock, mass fraction, LHV, HHV, and M_{db} of the specified feedstock type are specified in the study.

$$M_{wb} = \frac{M_{db}}{(1 + M_{db})} \quad (4.c)$$

where M_{wb} and M_{db} are the wet and dry basis moisture content in percent, respectively. Depending on the availability of comprehensive data sets, the HHV can alternatively be obtained for any feedstock type using equation (4.d) or (4.e).

$$HHV = LHV + 10.30\ (H_2 \times 8.94) \qquad (4.d)$$

$$HHV = 3.55C^2 - 232C - 2{,}230H + 51.2C \times H + 131N + 20{,}600 \qquad (4.e)$$

where HHV and LHV are the high and low heating values in British thermal units per pound (Btu/lb), respectively. H_2 is the fuel diatomic hydrogen in mass percent. H, C, and N are the hydrogen, carbon, and nitrogen dry biomass weight percent, respectively.

Generating Capacity and Combustion Type

The HRES tool offers four types of combustion systems for the wood and agricultural feedstocks, which range from a scale of 1 kW up to 150 MW with various output efficiencies. This comprises Bed combustors such as fluidized-bed combustors and fixed-bed combustors, which are the most expensive solutions in terms of capital cost, operational costs, and maintenance costs. Meanwhile, the most efficient solutions are in terms of output power and environmental pollution. The cyclone combustors are suitable for low-scale capacities, while the output power and environmental pollution efficiency are slightly lower than bed combustors. Lastly, the grate stokers combustors are generally the least expensive solutions, offering the least efficiency. On the other hand, for WtE incineration, the HRES offers fluidized-bed combustors and grate stokers combustors as the most popular technologies.

Energy Balance

The energy balance calculation follows the Btu method to obtain the energy balance; the efficiency losses of moisture in fuel, unburned fuel, dry flue gas losses, latent heat, moisture in the air, and miscellaneous manufacturing losses are estimated. The moisture in fuel losses is calculated using equation (4.f).

$$e_{fuel\,moisture} = M_{db} \frac{(H_2 - H_1)}{HHV} \qquad (4.f)$$

where $e_{fuel\ moisture}$ is the moisture in fuel losses in percent. H_1 and $H_2$are the water's enthalpy of the biomass at pre-combustion and the vaporized moisture enthalpy of the stack steam in Btu/lb, calculated using equations (4.g) and (4.h), respectively.

$$H_1 = T_A - 32 \tag{4.g}$$

$$H_2 = (0.00003958T_{FG} + 0.4329)T_{FG} + 1{,}062.2 \tag{4.h}$$

where T_A is the ambient temperature in Fahrenheit. $T_{FG}$is the steam leaving the stack temperature at the flue gas temperature, in Fahrenheit. The unburned fuel depends on the boiler type, which is a consequence of incomplete combustion due to the excess air amount. For well-maintained boilers and at acceptable excess air levels, the unburned fuel varies according to the technology, as demonstrated in equation (4.i).

$$\eta_{unburned\ carbon} = \begin{cases} 3.5\%\ for\ stoker\ boilers \\ 0.25\%\ for\ FBC \\ 3.0\%\ Cyclone \end{cases} \tag{4.i}$$

where $\eta_{unburned\ carbon}$ is the loss due to the unburned carbon in the fuel. The dry gas's mass flow rate is calculated using equation (4.j). Sequentially, the dry flue gas loss is calculated based on the temperature difference of the inlet air and the outlet steam leaving the stack at the flue gas temperature in Fahrenheit, as expressed in equation (4.k).

$$\dot{n} = \left(\left((12.7C + 38.1H) \times (1 + \frac{a}{100}\right) - 0.5O\right)\frac{1}{HHV} \tag{4.j}$$

$$e_{dry\ gas\ loss} = 24 \times (T_{FG} - T_A)\ \dot{n} \tag{4.k}$$

where $\dot{n}$ is the dry gas's mass flow rate in pounds per Btu fuel. a is the excess fed air based on the combustion system type, in percent. The latent heat losses generated due to the chemical reaction of the free hydrogen with the oxygen during the combustion are estimated from the generated steam during the combustion process using equation (4.l).

$$e_{latent\ heat} = \frac{H \times 100 \times 8.94}{HHV}\ (H_2 - H_1) \tag{4.l}$$

where $e_{latent\ heat}$ is the latent heat efficiency as a percentage of the total input heat. H_1 and H_2 are the water's enthalpy. The moisture in air losses are the spatiotemporal effects that vary with the geographical location and hourly climate parameters. In this model, the moisture in air losses is calculated using equation (4.m).

$$e_{moisture\ in\ air} = 45 \times \dot{n}\left(0.622 \times \left(\frac{(0.01 \times r \times P_{vd}}{P_b - (0.01 \times r \times P_{vd}}\right)\right)(T_{FG} - T_A) \qquad (4.m)$$

where $e_{moisture\ in\ air}$ is the moisture in air efficiency in percent. r is the relative humidity. $\dot{n}$ is the mass flow rate of dry gas. P_b denotes the barometric pressure, while P_{vd} is the saturated absolute pressure as calculated using equation 4.n):

$$P_{vd} = 0.0886e\left(\frac{17.2694T_c}{T_c + 238.3}\right) \qquad (4.n)$$

where P_{vd} is the water vapor's absolute saturated pressure in psi. T_c is the ambient temperature in Celsius.

Lastly, the manufacturer's margin losses are all lumped together. This includes radiation in the ash pit, sensible heat in ash, and sensible heat in flue dust. In this model, the manufacturer's margin losses are denoted by e_{manu} are assumed to be 2.03.

Mass Balance

The combustion system's mass balance is obtained through two material balances: the boiler steam and the biomass stream. After vaporization at the combustion stage, the useful heat is transferred to the feedwater in the boiler stream. Hence, since the generating plant capacity is given, the amount of heat is calculated by converting the generating capacity from kW to Btu and considering steam cycle and energy balance efficiencies as follows:

$$\dot{Q} = \frac{O_{Design} \times 3{,}412.14}{\eta_{steam\ cycle}} \times \left(\frac{\left(100 - \left(e_{fuel\ moisture} + e_{unburned\ carbon} + e_{dry\ gas\ loss} + e_{latent\ heat} + e_{moisture\ in\ air} + e_{manu}\right)\right)}{100} \right) \quad (4.\text{p})$$

where $\dot{Q}$ is the steam heat to be supplied to the turbine in Btu. O_{Design} is the generating capacity in kW. 3,412.14 is the kW-to-Btu conversion factor, while $\eta_{steam\ cycle}$ denotes the steam cycle efficiencies, normally assumed to be around 40%. $e_{fuel\ moisture}$, $e_{unburned\ carbon}$, $e_{dry\ gas\ loss}$, $e_{latent\ heat}$, $e_{moisture\ in\ air}$, and e_{manu} are the efficiency losses representing the heat loss due to the energy balance. Using the obtained steam heat to be supplied to the turbine, the biomass feeding rate can be calculated using equation (4.q).

$$\dot{b} = \frac{\dot{Q}}{HHV \times \left(\frac{\left(100 - \left(e_{moisture\ in\ air} + e_{latent\ heat} + e_{fuel\ moisture} + e_{manu} + e_{rad} + e_{dry\ gas\ loss}\right)\right)}{100} \right)} \quad (4.q)$$

where $\dot{b}$ is the biomass feeding rate in lb/hr. HHV is the feedstock gross calorific value. Consequently, by obtaining the heat transferred to the feedwater boiler and the biomass feeding rate, the net annual biomass-generated electricity is calculated as expressed in equation (4.r).

$$O_{net} = \frac{\left(\sum_{0}^{8760} \dot{Q} \times \ \eta_{steam\ cycle} \times \ t \right)}{3{,}412.14} \quad (4.r)$$

where O_{net} is the net annual output of the biomass generator in kWh. t denotes the time interval of one hour.

Biomass output parameters

The power plant's parasitic load is the self-consumption required by the operation (i.e., pumps, electronic control, motors, and on-site miscellaneous loads), which is usually assumed to be between 10 and 15 percent. This study considers the parasitic 10 percent load of the net generated electric energy. The total generated energy in kWh is calculated considering the net generated power and parasitic load from the relation expressed in equation (4.s).

$$O_{net} = O_{gross} \times \left(1 - \frac{P}{100}\right) \quad (4.s)$$

where O_{gross} is the total generated energy in kWh, and O_{net} is the net generated energy considering the parasitic load P in percent. On the other hand, the heat rate (MMBtu/MWh), thermal efficiency in percent, capacity factor in percent, hourly net generated energy in kWh, and the annual generated energy in kWh are calculated using equations (4.t) to (4.x), respectively.

$$HR_{gross} = \frac{\dot{b} \times HHV}{O_{net} \times 1000} \quad (4.t)$$

$$HR_{net} = \frac{\dot{b} \times LHV}{O_{net} \times 1000} \quad (4.u)$$

$$\eta_{therm,HHV} = \frac{341.23}{HR_{gross}} \quad (4.v)$$

$$\eta_{therm,LHV} = \frac{341.23}{HR_{net}} \quad (4.w)$$

$$CF = \frac{O_{net}}{C_{design} \times 8760} \quad (4.x)$$

where the gross heat rate HR_{gross} in MMBtu/MWh is calculated using equation (4.t), considering the amount of biomass feeding rate in lb/year, HHV, and the net annual output energy. Equation (4.u) calculates the net heat rate. HR_{net} in MMBtu/MWh, considering the LHV. Furthermore, the thermal efficiency at HHV $\eta_{therm,HHV}$ and at LHV $\eta_{therm,LHV}$ are calculated using equations (4.v) and (4.w), in percent, respectively. Eventually, the capacity factor in percent is calculated.

5. Energy Storage Cycles of Electric Batteries:

The charging and discharging cycles are based on the given technology and initial charging state. The energy storage of electric batteries is restricted to off-grid mode and with disabled biomass generation. The conditions of charging and discharging cycles are expressed in equations (5.a) and (5.b), respectively.

$$E_{PV_t} + E_{WT_t} > E_{Load_t} \tag{5.a}$$

$$E_{PV_t} + E_{WT_t} < E_{Load_t} \tag{5.b}$$

$$E_{CD_t} = E_{PV_t} + E_{WT_t} - E_{Load_t} \tag{5.c}$$

where E_{PV_t} is the hourly generated electricity from solar panels for the time step of t in kWh. E_{WT_t} is the hourly generated electricity from wind in kWh. E_{Load_t} is the hourly electricity demand in kWh. E_{CD_t} is the charged or discharged amount of battery energy, whereas the negative sign indicates the discharging direction. The surplus power from the renewable energy supply aims to charge the batteries, while during the supply shortage, the batteries discharge to support the renewable energy supply. The rated power of the battery energy storage is sized based on the peak load of the HRES as expressed in equation (5.d). The batteries' state of charge is constrained to be between a minimum discharging level of more than 20% and a maximum charging level of below 80% to maximize the efficiency and lifetime of the batteries. Hence, the hourly state of charge is calculated as formulated in equation (5.d).

$$P_R = \frac{E_{L,Max} \cdot AD}{DOD.\eta_b} \tag{5.d}$$

$$20\% < SOC_t < 80\% \tag{5.e}$$

$$SOC_t = SOC_{t-1} + \frac{E_{CD_t}\,\eta_{inv}}{P_R} \tag{5.f}$$

Where P_R is the size of the rated power capacity of the battery in kWh. $E_{L,Max}$ is the peak demand load in kWh. AD is the autonomy days of the batteries, which is the time period the battery can meet the demand without a charging event. The sizing of all battery technologies is modeled by considering three days of autonomy. DOD is the depth of discharge in percent, which varies according to the technology and manufacturer. The technical specification of the applied battery. η_b and η_{inv} are the battery round-trip efficiency and inverter efficiency in percent, respectively.

6. Pollutant concentrations change using a dispersion model

The dispersion model employs a steady-state Gaussian dispersion model to estimate the hourly concentration at downwind distance, x, in km and the crosswind distance, y, in km.

$$C = \frac{QH}{2\pi v_s \delta_y \delta_z} exp\left[-0.5\left(\frac{y}{\delta_y}\right)^2\right] \tag{6.a}$$

$$H = \left[exp\left(-0.5\left(\frac{z-h}{\delta_z}\right)^2\right)\right] + \left[exp\left(-0.5\left(\frac{z+h}{\delta_z}\right)^2\right)\right] \tag{6.b}$$

$$\delta_y = 465.12xtan(0.0174(\theta - \mu\, ln(x)) \tag{6.c}$$

$$\delta_z = \partial x^{\rho} \tag{6.d}$$

$$v_s = v_0 \left(\frac{H}{z_0}\right)^p \tag{6.e}$$

where, C is the concentration in g/m^3. E is the emission rate of the pollutant. $v_s$is the average wind speed at the height of release in m/s. z is the height of the receptor in meters. δ_y and δ_z are the standard deviations of concentration distribution for the lateral and vertical directions in meters, respectively. h is the height of the effective source, with respect to the vertical distance between the ground and the exhaust pipe. θ, μ, ∂ , and ρ are the constant coefficients, which are defined according to the given values of the local area's stability category. x is the source distance in meters.

7. Potential Reduction in GHG Emissions and Air Pollutants

The viability of the avoided emissions stems from estimating the substitution of the polluted electric energy of the national grid with cleaner HRES electricity. This is mathematically expressed using Equations (7.a)–(7.c).

$$AE = (E_T - E_c) \times EF_{p,grid} \tag{7.a}$$

$$E_T = \sum_t \sum_\tau E_{\tau,t} \tag{7.b}$$

$$E_c = \sum_t \sum_\tau C_{\tau,t} \tag{7.c}$$

where AE is the annual avoided GHG emissions and air pollutants in tons per year. E_T and E_c are the annual total electricity generation and the annual self-electricity consumption of the proposed HRES per year, respectively. $EF_{p,grid}$ is the electricity grid's pollutant emission factors. $E_{\tau,t}$ is the hourly electricity generation per technology τ (i.e., solar, wind, biomass, and battery). $C_{\tau,t}$ is the hourly self-electricity consumption of technology τ.

8. Public Health Co-Benefit Assessment

The proposed methodology in this research uses DALYs to indicate the mortality caused by the different diseases. DALYs are defined as the total of years of potential life lost from premature death and disability-related diseases. The percentage change in the health outcome for each unit change in $PM_{2.5}$ concentration is used to calculate the effect estimates for DALYs. The health burden of the population was obtained based on selected diseases for the exposure group in the targeted locus of Japan. The diseases encompass chronic obstructive pulmonary disease (COD), ischemic heart disease (IHD), cerebrovascular disease (Stroke), lung cancer (LC), tuberculosis and bronchus (TB), and acute lower respiratory infections (ALRI). The relative risk of the exposure level of interest for the subject diseases is a function of the health response to a change in $PM_{2.5}$ concentration per pollutant concentration, and the pollutant concentrations change with respect to the baseline indices, as expressed in Equation (8.a).

$$RR_{m,n} = \text{f}(\beta, \Delta C_{PM}) \tag{8.a}$$

where $RR_{m,n}$ is the relative risk of the exposure level of interest for the subject diseases. β is the coefficient of the health response to a change in $PM_{2.5}$ concentration. ΔC_{PM} is the change in pollutant concentrations with respect to the baseline indices. In this study, a dispersion model is developed to find the change in pollutant concentrations, considering the baseline concentration of $PM_{2.5}$ as the major air pollutant. m and n are the selected disease and the exposure group, respectively. Sequentially, based on the obtained relative risk, the population-attributable risk fraction ($PAF_{m,n}$) for the selected disease was calculated using Equation (8.b).

$$PAF_{m,n} = \frac{RR_{m,n} - 1}{RR_{m,n}} \tag{8.b}$$

The overall mortality and morbidity are measured using the following equations:

$$ADALYs_{m,n} = (DALYs_{m,n,base} \times PAF_{m,n,base}) - (DALYs_{m,n,int} \times PAF_{m,n,int}) \tag{8.c}$$

where $DALYs_{m,n}$ is the DALYs attributable to the selected disease (m) in the exposure group (n). $ADALYs_{m,n}$ is the DALYs averted from the intervention scenario, after deploying the proposed HRES. base and int denote baseline and intervention scenarios. The values of the $DALYs_{m,n,base}$ for the selected diseases are obtained. The monetized benefits of averted DALYs can be estimated based on the per capita gross domestic product (PGDP) that an individual with a healthy life can achieve in one year:

$$AVC_{n,m} = PGDP \times ADALYs_{m,n} \tag{8.d}$$

where $AVC_{n,m}$ represents the avoided cost of mortality and morbidity due to averted DALYs in a year.

9. Cost-benefit Assessment

The profitability of the intervention scenarios was investigated through the economic feasibility of implementing the HRES resources. This includes the net profit values, payback period, and marginal abatement cost. In this tool, the amount of energy imported from the national grid to balance the unmet demand of HRES was considered a purchasing expense, while the surplus energy exported to the national grid was considered revenue. Given this, the cost–benefit analysis of integrating the HRES can be exploited as expressed in Equations (9.a)–(9.e)

$$NPV = \sum_{t=1}^{T} \frac{R_t}{(1+r)^t} - C \tag{9.a}$$

$$R_t = (AS_t - CE_t) \tag{9.b}$$

$$AS_t = AS_{Elctricity,t} + AS_{Co-benefits,t} \tag{9.c}$$

where NPV is the net present value calculated for the period of the project lifetime. R_t represents the cash flow at year t, which is calculated by subtracting the outflow cash from the inflow cash. C is the total capital and installation costs. T is the project lifetime, and r is the discount rate. AS_t is the incoming cash flow, which includes the revenues from selling electricity to the HRES's end customers and the national grid, as denoted by $AS_{Elctricity,t}$. In addition, the monetized health co-benefits (AVC) as obtained in the previous section are included in the incoming cash flow calculation, which is denoted by $AS_{Co-benefits,t}$. CE_t is the cash outflow, including fixed, operational, and maintenance costs. Sequentially, the payback period of the utilized HRES was calculated annually considering the total capital and installation costs, and the marginal annual cash flow is shown in Equation (9.a) and Equation (9.d), respectively. The marginal abatement cost of the total GHG emissions abated over the project lifetime was calculated as expressed in Equation (9.e).

$$PBP = \sum_{t=1}^{T} \frac{C}{\frac{R_t}{(1+r)^t}} \tag{9.d}$$

$$MAC = \frac{-NPV}{TEA} \tag{9.e}$$

where PBP is the payback period calculated per annum. MAC is the marginal abatement cost in USD per ton of GHG emissions abated. TEA is the cumulative GHG emissions abated over the project lifetime in tons.

10. Green job and economy

The integration of the Matching model, Cobb-Douglas production model, and the Leontief input-output (I-O) model is achieved by acquisition of data from Input-Output tables and the supply-use tables. The tables comprise a sector-to-sector matrix of 45 by 45 quantifying economic interrelationships, illustrating producer-consumer linkages. This dataset offers statistics and charts for analyzing internal and cross-border production and consumption in the Philippines at local, regional, and global levels. Processing these data leads to the extraction of an employment factor coefficient, $J_{C_{ik}}$ and green economy coefficient $E_{C_{ik}}$ for solar energy. Figure 3 illustrates the overall methodological flowchart.

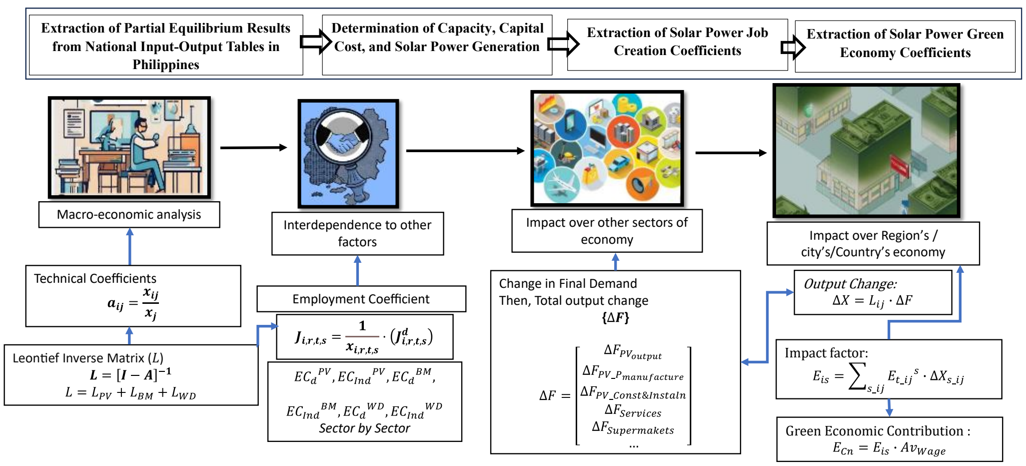

Figure 3: Overall methodological flowchart expanded from the National Input-Output table to estimate job creation and green economy coefficient

The employment coefficient is calculated through sequential formulation. J_T is the coefficient considered in equation (10.a) to determine the total number of jobs created in each project scenario. J_{PV} denotes the employment coefficient for solar power, P_{PV} is the generated electricity from the solar power project.

$$J_T = J_{PV} \cdot P_{PV} \tag{10.a}$$

The production equation, based on the Cobb-Douglas production model, is formulated for n sectors within a specified region, r. This formulation ensures alignment with the production balance and corresponds to the structure of the input-output table as follows:

$$X = [I - A]^{-1} \cdot y \tag{10.b}$$

Where X and A represents the total output per sector, while the sector-by-sector, nxn, are the intermediate input coefficient matrix of one region, with each element of $A_{i,j}$ displaying the intermediate input needed from sector i to generate one unit of the final product of sector j, respectively. y is the total final demand vector. Sequentially, the resulting equilibrium is transformed into a system of linear equations, incorporating weighted values derived from the input-output tables. These weighted values reflect sectoral interdependencies and economic contributions, enhancing the accuracy of the equilibrium representation. The system is then augmented into a matrix form, as expressed in equation (10.c):

$$\begin{bmatrix} x^1 \\ x^2 \\ x^3 \\ x^4 \\ x^5 \end{bmatrix} = \left[I - \begin{bmatrix} A^{11} & A^{12} & A^{13} & A^{14} \\ A^{21} & A^{22} & A^{23} & A^{24} \\ A^{31} & A^{32} & A^{33} & A^{34} \\ A^{41} & A^{42} & A^{43} & A^{44} \\ A^{51} & A^{52} & A^{53} & A^{54} \end{bmatrix} \right]^{-1} \begin{bmatrix} y^1 \\ y^2 \\ y^3 \\ y^4 \\ y^5 \end{bmatrix} \qquad (10.c)$$

The counters from 1 to 5 represent the construction of solar power facilities, operation of solar power facilities, Solar power electricity contribution to indirect sectors, other renewable energy power generation, and non-electricity sectors that are indirectly related to solar power. This shows the inter-sectoral transactions within a single region, driven by solar power generation activities, which enable the calculation of a distinct employment coefficient. The input from other sectors to support solar power generation serves the requirements of the different sectors as catered in $A^{n,i}x^{n,j}$(e.g., $A^{11}x^1$). This coefficient solely depends on the solar power generation capacity in the form of construction, operational, and indirectly related sectors to determine the potential number of jobs generated. The Leontief Inverse Matrix (the total requirements matrix) is applied in the input-output analysis. This matrix illustrates the quantity of gross output from sector i needed to fulfill one unit of final demand y from sector j. Sequentially, the job creation coefficient is calculated by matching ($J_{i,r,t,s}$), formed in the i^{th} sector, in the region, r, in year, t, under scenario, r, as expressed by (10.d):

$$J_{i,r,t,s} = \frac{1}{x_{i,r,t,s}} \cdot (J^d_{i,r,t,s}) \qquad (10.\mathrm{d})$$

Where $J^{d}_{i,r,t,s}$ are the regular direct employment opportunities in the i^{th} sector, in region r for year t under scenario s. $x_{i,r,t,s}$ is the total production output. The values for $J^{d}_{i,r,t,s}$ are obtained from the input-output table. The employment coefficient, J_{C_i} is determined by solving the linear system of equations expressed in (10.e):

$$J_T = \begin{bmatrix} J_{C_1} \\ J_{C_2} \\ J_{C_3} \\ J_{C_4} \\ J_{C_5} \end{bmatrix} \left[I - \begin{bmatrix} A^{11} & A^{12} & A^{13} & A^{14} \\ A^{21} & A^{22} & A^{23} & A^{24} \\ A^{31} & A^{32} & A^{33} & A^{34} \\ A^{41} & A^{42} & A^{43} & A^{44} \\ A^{51} & A^{52} & A^{53} & A^{54} \end{bmatrix} \right]^{-1} \begin{bmatrix} y^1 & & & & \\ & y^2 & & & \\ & & y^3 & & \\ & & & y^4 & \\ & & & & y^5 \end{bmatrix} \qquad (10.e)$$

Where y^n is the share of the ultimate demand allocated to a sector, calculated using the capital cost of the associated sector, employment value relative to the sector, and the wage for a regular employee within the sector.

$$y^{ni} = \frac{1}{x^{ni}}\left(e^i * w^i\right) \qquad (10.\mathrm{f})$$

Where x^{ni} is the capital cost of sector i. e^i is the employment value in the sector. w^i is the wage for a regular employee within the sector. The economic contribution reveals how wages spent by green job workers circulate through the economy, affecting various sectors, and driving demand for goods and services. Construction of renewable energy projects generates employment for engineers, electricians, and laborers, while procurement of sustainable materials benefits manufacturers and suppliers. Operations and maintenance create long-term jobs for technicians and system operators, ensuring efficiency in solar power generation systems. Indirect employment emerges to offer crucial support in areas such as consulting, finance, legal services, and supply chain management, further amplifying economic activity. The green economy therefore strengthens supply chains, boosting job creation in manufacturing, logistics, and technology. The workers' earnings support businesses in retail, healthcare, and real estate, creating economic resilience and growth. In this report, a comprehensive monetary assessment highlights how green jobs in solar system projects drive economic growth, enhance sustainability, and foster a more resilient and robust economy. The formulation of green economy contributions maintains consistency with production equilibrium and aligns systematically with the structural framework of the input-output table as follows:

$$S_V = (I - A)^{-1} \cdot f \qquad (10.\mathrm{g})$$

Where $S_V, A\ and\ f$ represents the total output vector for the solar sector, technical coefficient matrix, and final demand vector, respectively. This corresponds to the Leontief inverse matrix (L) illustrated by equation (10.h). The change in the final demand (ΔF_s) in solar energy employment is based on equation (10.i), while the solar energy employment green economic coefficient (E_{is}) is tabulated as a function of the annual income multiplier per person employed in the sector (${E_{t\_ij}}^{s}$) obtained from equation (10.j). The green economy contribution E_{Cn}, for solar energy employment is therefore expressed according to equation (10.k).

$$L = (I - A)^{-1} \tag{5.1h}$$

$$\Delta X = L_{ij} \cdot \Delta F \tag{5.1i}$$

$$E_{is} = \sum\nolimits_{s\_ij} {E_{t\_ij}}^{s} \cdot \Delta X_{s\_ij} \tag{5.1j}$$

$$E_{Cn} = E_{is} \cdot Av_{Wage} \tag{5.1k}$$

The overall back-end modeling flowchart of the activity parameters is depicted in Figure 4 below; the detailed calculation methodologies are as explained in the preceding sections.

11. Electric Load Types

The load types in the developed methodology are typical patterns of residential, commercial, and community loads, as depicted in Figure 4. Equation (11.a) aligns the deviation of the default hourly amount of load patterns with the actual per capita capacity consumption by calculating the load adjustment factor. The load adjustment factor is then employed to determine the system's annual demand as expressed in equation (11.b).

$$LAF = \frac{PCC}{\sum_{t=1}^{8760} Load\ Pattern} \tag{11.a}$$

$$\sum_{t=1}^{8760} Demand = LAF \cdot \sum_{t=1}^{8760} Load\ Pattern \tag{11.b}$$

where LAF is the load adjustment factor, PCC is the per capita capacity consumption, and $Load\ Pattern$ denotes the default hourly load patterns, which can be selected from one of the typical patterns of residential, commercial, or community loads. t is the hourly time step interval.

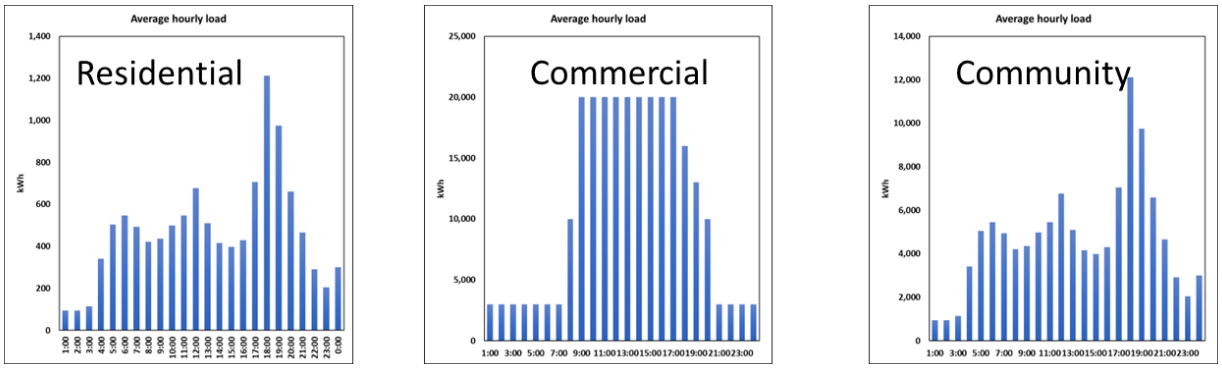

Figure 4: Representation of the default typical load patterns

On the other hand, the number of load units for intervention scenarios is calculated based on the annual supply from the HRES to the per capita capacity consumption as expressed in equation (5.2c). Given this, the hourly annual demand is employed to calculate the load factor, peak, annual, daily, hourly, and average demand. However, the electric load modeling has the limitation of combining different types of loads. Thus, the investigated intervention scenarios are limited to residential load patterns.

$$Number\ of\ load\ units = \frac{\sum_{t=1}^{8760} HRES\ Supply}{PCC} \qquad (10.c)$$

References:

[1] Farzaneh H., Dashti M., Zusman E., Lee S-Y., Dagvadorj D., Nie Z. (2022). Assessing the Environmental-Health-Economic Co-Benefits from Solar Electricity and Thermal Heating in Ulaanbaatar, Mongolia. International Journal of Environmental Research and Public Health, 19(11):6931

[2] Suliman M., Farzaneh H., Zusman E., Mulumba A., Lestar P., Permadi P.A. and JanardhananN. (2024). Quantifying the Climate Co-Benefits of Hybrid Renewable Power Generation in Indonesia: A Multi-Regional and Technological Assessment, Climate, 12(2), 23

Further References:

- Farzaneh,H., Zusman,E., Chae,Y.(2021). Aligning Climate Change and Sustainable Development Policies in Asia, Springer.
- Farzaneh,H.(2019).Energy systems modeling:Principles and applications, Springer.
- Farzaneh,H. (2018). Devising a clean energy strategy for Asian cities, Springer.
- Joshi, S., Sukhwani, V., Mitra, B.K., Deshkar, M.S., Suliman, S.M., Moradi, M., Mulumba, A., Zusman, E., Farzaneh, H. (2026). Harnessing agrivoltaics for healthy net-zero transition in Nagpur, India: geospatial suitability and co-benefits assessment, Sustainability Science
- Mohammed, R.K., Farzaneh, H. (2024). Quantifying the multiple environmental, health, and economic co-benefits from the adoption of carbon capture technology in the power sector in southern Iraq, using a recurrent neural network-based health assessment approach, Journal of Environmental Management, 121848
- Hassan Bhat,T., Farzaneh, H., Toosty, N.T. (2022). Co-Benefit Assessment of Active Transportation in Delhi, Estimating the Willingness to Use Nonmotorized Mode and Near-Roadway-Avoided PM2.5 Exposure, International Journal of Environmental Research and Public Health: 19(22), 14974
- Hassan Bhat,T., Farzaneh, H.(2022). Quantifying the multiple environmental, health and economic benefits from the electrification of the Delhi public transport bus fleet, estimating a district-wise near roadway avoided PM2.5 exposure, Journal of Environmental Management:116027
- Jiawen, G.; Huijuan, D.; Farzaneh, H.; Yong, G.; Reddington, C. (2022). Uncovering the overcapacity feature of China's industry and the environmental & health co-benefits from de-capacity. Journal of Environmental Management, 308, 114645
- Hassan Bhat, T., Jiawen, G., Farzaneh, H. (2021). Air Pollution Health Risk Assessment (AP-HRA), Principles and Applications. Int. J. Environ. Res. Public Health, 18, 1935.
- Gómez-Sanabria, A., Zusman, E., Höglund-Isaksson, L., Klimont, Z., Lee, S., Akahoshi, K., Farzaneh, H., & Chairunnisa. (2020). Sustainable wastewater management in Indonesia's fish processing industry: Bringing governance into scenario analysis. Journal of Environmental Management, 111241.

- Farzaneh, H., De Oliveira, J. A., McLellan, B., & Ohgaki, H. (2019). Towards a low emission transport system: Evaluating the public health and environmental benefits. Energies, 12(19), 3747.